Thermochimica Acta, 184 (1991) 9–23
Elsevier Science Publishers B.V., Amsterdam

Kinetics of dehydration of sodium salt hydrates

S.K. Sharma, C.K. Jotshi and Suniti Kumar

Energy Research Centre, Punjab University, Chandigarh, 160014 (India)

(Received 8 October 1990)

Abstract

The kinetics of dehydration of sodium salt hydrates, namely sodium acetate trihydrate, sodium thiosulphate pentahydrate and disodium hydrogen phosphate dodecahydrate are reported. These salt hydrates have been recommended for thermal energy storage applications. The kinetic analysis was carried out on a simultaneous DTA/TG apparatus. Kinetic parameters were evaluated from TG data. Ten models of possible controlling mechanisms have been considered for the determination of kinetic parameters. Results show that in these cases it is difficult to select a suitable mechanism for the determination of kinetic parameters using the best fit straight line method suggested by Coats and Redfern and the minimum standard deviation method suggested by Zsako. A new criterion is proposed in this work for the selection of a suitable mechanism.

LIST OF SYMBOLS

c'	constant in eqn. (10)
E_{act}	energy of activation (kJ mol^{-1})
ΔH	enthalpy of dehydration (kJ mol^{-1})
q	heating rate (K min^{-1})
R	gas constant
t	time
T	absolute temperature
w_0	weight at the start of the step
w_c	weight at the end of the step
w_T	weight at temperature T
Z	pre-exponential factor
α	fractional decomposition $(w_0 - w_T)/(w_0 - w_c)$
$f(\alpha)$	equation representing the controlling mechanism as shown in Table 1

INTRODUCTION

Hydrated sodium salts have been recommended for thermal energy storage applications [1,2]. However, these salts suffer from two major problems:

0040-6031/91/$03.50

supercooling and phase segregation. Supercooling can be reduced to a large extent by using nucleating agents [2], but problems associated with phase segregation have not been fully solved. This has hampered the large-scale use of these salts for storage applications. Phase segregation takes place mainly due to (i) formation of lower salt hydrates during the heating and cooling cycles, (ii) loss of water of crystallization during heating and (iii) decrease in the solubility of anhydrous salt with increase in temperature above the transition temperature, eg. in the cases of $Na_2SO_4 \cdot 10H_2O$ and $Na_2CO_3 \cdot 10H_2O$.

TABLE 1

Mathematical expression of the functions $f(\alpha)$ and $g(\alpha)$

Controlling mechanism	Symbol	$f(\alpha)$	$g(\alpha)$
Nucleation and nuclei growth			
A. Extremely rapid nucleation followed by rapid growth			
Linear advance of interface (one-dimensional)	R_1	1	
Two-dimensional (expanding or contracting cylinder)	R_2	$(1-\alpha)^{1/2}$	$2[1-(1-\alpha)^{1/2}]$
Three-dimensional (expanding or contracting sphere)	R_3	$(1-\alpha)^{2/3}$	$3[1-(1-\alpha)^{1/3}]$
B. Ingestion of nucleus sites, overlapping of growth nuclei			
Random nucleation (Mampel unimolecular law)	F_1	$(1-\alpha)$	$-\ln(1-\alpha)$
Avrami–Erofeev nuclei growth			
Two-dimensional growth	A_2	$2[-\ln(1-\alpha)^{1/2}](1-\alpha)$	$[-\ln(1-\alpha)]^{1/2}$
Three-dimensional growth	A_3	$3[-\ln(1-\alpha)^{1/3}](1-\alpha)$	$[-\ln(1-\alpha)]^{1/3}$
Diffusion			
Parabolic law (one-dimensional transport process)	D_1	$1/2\alpha$	α^2
Two-dimensional diffusion	D_2	$[-\ln(1-\alpha)^{-1}]$	$(1-\alpha)\ln(1-\alpha)+\alpha$
Three-dimensional diffusion (Jander mechanism)	D_3	$1.5\left\{\frac{(1-\alpha)^{2/3}}{[1-(1-\alpha)^{2/3}]}\right\}$	$[1-(1-\alpha)^{1/3}]^2$
Three-dimensional diffusion (Brounshtein–Ginstling mechanism)	D_4	$1.5\left\{\frac{1}{(1-\alpha)^{-1/3}-1}\right\}$	$(1-2\alpha/3)-(1-\alpha)^{2/3}$

In this study an attempt has been made to evaluate the loss of water of crystallization during the heating cycle as this is one of the important parameters associated with phase segregation. The mechanism and energy of activation have been determined using the thermogravimetric (TG) technique.

Integral methods have been reported to give better results than differential and approximate methods [3] for the evaluation of kinetic parameters. In the present study, two techniques based on the integral methods of Coats and Redfern [4] and of Zsako [5] were used to determine kinetic parameters from TG data. The different mechanisms of the solid state reactions considered in the present work are reported in Table 1 [6,7].

EXPERIMENTAL

Sodium acetate trihydrate ($NaCH_3COO \cdot 3H_2O$) and sodium thiosulphate pentahydrate ($Na_2S_2O_3 \cdot 5H_2O$) were recrystallized from laboratory grade reagents, using doubly distilled water. Disodium hydrogen phosphate dodecahydrate ($Na_2HPO_4 \cdot 12H_2O$) was crystallized from anhydrous disodium hydrogen phosphate. The compositions of the basic salts used are given below.

Sodium acetate trihydrate. Minimum assay 99%, pH (5% solution) 7–9. Maximum limit of impurities: chloride (Cl), 0.001%; sulphate (SO_4), 0.005%; heavy metals as (Pb), 0.002%; iron (Fe), 0.002%; calcium (Ca), 0.005%; potassium (K), 0.05%. Manufactured by E. Merck (India).

Sodium thiosulphate pentahydrate. Minimum assay 99%, pH (5% solution) 5.5–7.5. Maximum limits of impurities: chloride (Cl), 0.02%; sulphate and sulphite as (SO_4), 0.01%; sulphide (S), 0.001%; heavy metals (Pb), 0.001%; iron (Fe), 0.005%; calcium (Ca), 0.01%. Manufactured by E. Merck (India).

Disodium hydrogen phosphate. Minimum assay (after drying) 99.5%, pH of solution 9.0–9.2. Maximum limit of impurities: insoluble matter, 0.01%; chloride (Cl), 0.002%; nitrogen compounds, 0.002%. Manufactured by E. Merck (India).

Thermal analysis of the hydrated salts was carried out on a MOM Derivatograph (Budapest) which is a simultaneous thermal analyser. Heating was carried out at a linear rate of 5 K min^{-1}. Heating was continued up to the total loss of water of crystallization only.

RESULTS AND DISCUSSION

Thermograms (DTA/TG curves) of the salts $NaCH_3COO \cdot 3H_2O$, $Na_2S_2O_3 \cdot 5H_2O$ and $Na_2HPO_4 \cdot 12H_2O$ are shown in Figs. 1–3. Dehydra-

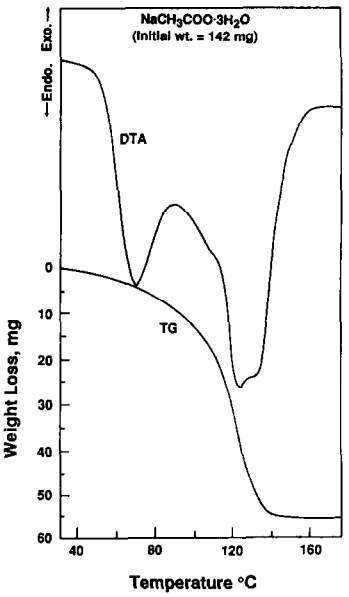

Fig. 1. Thermogram of $NaCH_3COO \cdot 3H_2O$.

tion of these hydrates was continued until they had completely lost their water of crystallization. The number of DTA peaks which appear during the dehydration reaction are reported in Table 2. The DTA peaks demonstrate that the melting and dehydration of the hydrates is, as expected, an

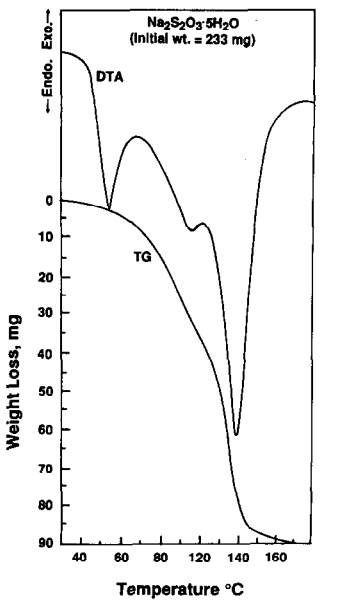

Fig. 2. Thermogram of $Na_2S_2O_3 \cdot 5H_2O$.

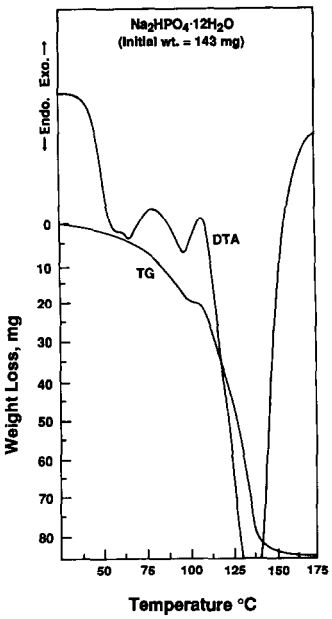

Fig. 3. Thermogram of $Na_2HPO_4 \cdot 12H_2O$.

endothermic process. The first DTA peak is due to melting of the hydrate, and the subsequent peaks are due to their dehydration. It can be observed from the DTA peaks that the dehydration process occurs with or without the formation of intermediate salt hydrates. In the case of $NaCH_3COO \cdot 3H_2O$, dehydration takes place in one stage only, i.e. without the formation of a lower hydrate. In the thermogram of this hydrate, only two DTA peaks are observed, one corresponding to the phase change of the salt hydrate and the second to the dehydration. In the thermograms of $Na_2S_2O_3 \cdot 5H_2O$ and $Na_2HPO_4 \cdot 12H_2O$, at least two endothermic DTA peaks are observed after the melting peaks. This shows that dehydration of these salts takes place in two stages. It can also be observed from the thermograms of these salt hydrates that there is a change in shape of the TG curves corresponding to

TABLE 2

DTA peaks and corresponding thermal phenomenon

Salt hydrate	Number of peaks	Thermal phenomenon
$NaCH_3COO \cdot 3H_2O$	2	Melting
		Dehydration
$Na_2S_2O_3 \cdot 5H_2O$	3	Melting
		Dehydration 1st step
		Dehydration 2nd step
$Na_2HPO_4 \cdot 12H_2O$	3	Dehydration 1st step
		Dehydration 2nd step

the DTA peaks, which also confirms the stepwise dehydration. On the basis of the water-loss calculations from the TG curves, the hydrates undergo the following transitions as represented by the second and third DTA peaks:

$$NaCH_3COO \cdot 3H_2O \rightarrow NaCH_3COO + 3H_2O\uparrow \quad (1)$$

$$Na_2S_2O_3 \cdot 5H_2O \rightarrow Na_2S_2O_3 \cdot 3H_2O + 2H_2O\uparrow \quad \text{(1st transition)} \quad (2)$$

$$Na_2S_2O_3 \cdot 3H_2O \rightarrow Na_2S_2O_3 + 3H_2O\uparrow \quad \text{(2nd transition)} \quad (3)$$

$$Na_2HPO_4 \cdot 12H_2O \rightarrow Na_2HPO_4 \cdot 9.5H_2O + 2.5H_2O\uparrow \quad \text{(1st transition)} \quad (4)$$

$$Na_2HPO_4 \cdot 9.5H_2O \rightarrow Na_2HPO_4 + 9.5H_2O\uparrow \quad \text{(2nd transition)} \quad (5)$$

In this study, two techniques based on the integral method have been used to determine the rate-controlling mechanisms and the corresponding kinetic parameters: the Coats–Redfern and Zsako methods. The kinetic parameters of the dehydration of $NaCH_3COO \cdot 3H_2O$, $Na_2S_2O_3 \cdot 5H_2O$ and $Na_2HPO_4 \cdot 12H_2O$ have been determined by these two techniques.

Coats–Redfern method

According to the modified Coats–Redfern equation [7]

$$\log[g(\alpha)/T^2] = \log[(ZR)/(E_{act}q)] - E_{act}/2.303RT \quad (6)$$

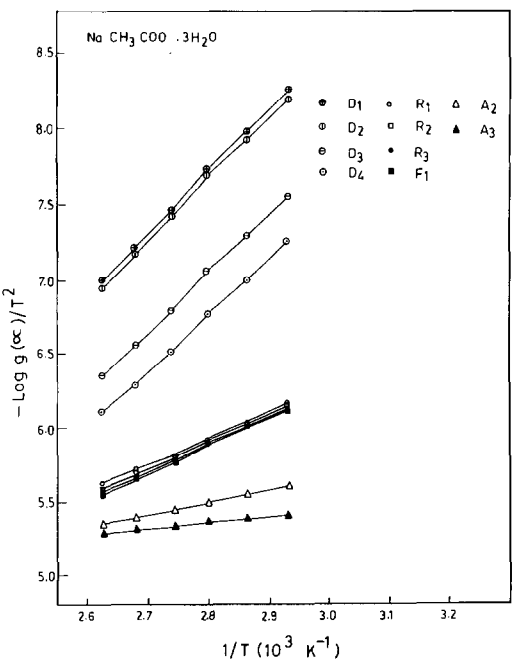

Fig. 4. Plot of $-\log[g(\alpha)/T^2]$ vs. $1/T$ for $NaCH_3COO \cdot 3H_2O$.

where

$$g(\alpha) = \int_0^{\alpha} d\alpha/f(\alpha) \tag{7}$$

The best straight line in the plot of $\log[g(\alpha)/T^2]$ vs. $1/T$ determines the mechanism and gives a unique value for the energy of activation. Plots of $\log[g(\alpha)/T^2]$ vs. $1/T$ for the possible controlling mechanisms of the dehydration of the salt hydrates are shown in Figs. 4–8. It can be observed from these figures that more than one straight line fits the experimental data. The mechanisms R_1, R_2, R_3 and F_1 give one set of nearly straight lines; similarly, the mechanisms D_1, D_2, D_3 and D_4 give another set of nearly straight lines. However, the deviation from a perfect straight line is greater for the second than for the first set of mechanisms. The Avrami–Erofeev mechanisms, A_2 and A_3, also show a linear relationship. The energy of activation values obtained from the slope of these straight line are reported in Tables 3–7 under the heading Coats–Redfern. It can be observed from these tables that the energy of activation does not vary much for a family of lines. However, the activation energy values vary considerably for the different mechanisms. For example, the Avrami–Erofeev mechanism gives the lowest activation energy values and the diffusion mechanism gives the highest. The values for the other mechanisms fall between those of the Avrami–Erofeev and the diffusion mechanism. It is interesting to note that the various equations representing the rate-controlling mechanisms yield

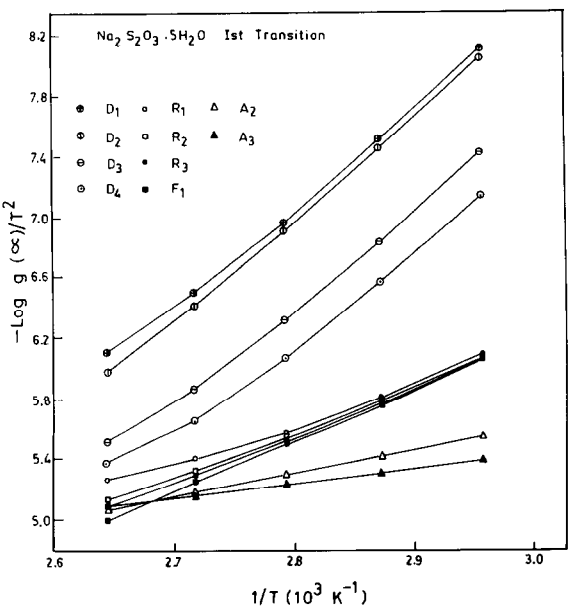

Fig. 5. Plot of $-\log[g(\alpha)/T^2]$ vs. $1/T$ for $Na_2S_2O_3 \cdot 5H_2O$ (1st transition).

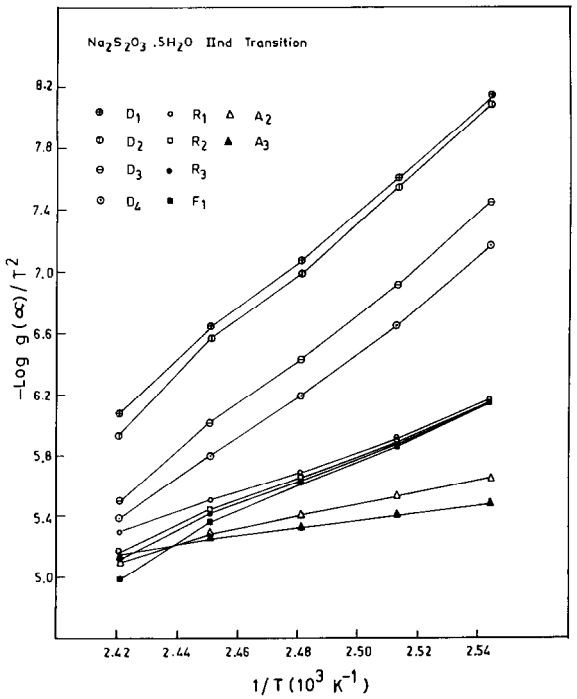

Fig. 6. Plot of $-\log[g(\alpha)/T^2]$ vs. $1/T$ for $Na_2S_2O_3 \cdot 5H_2O$ (2nd transition).

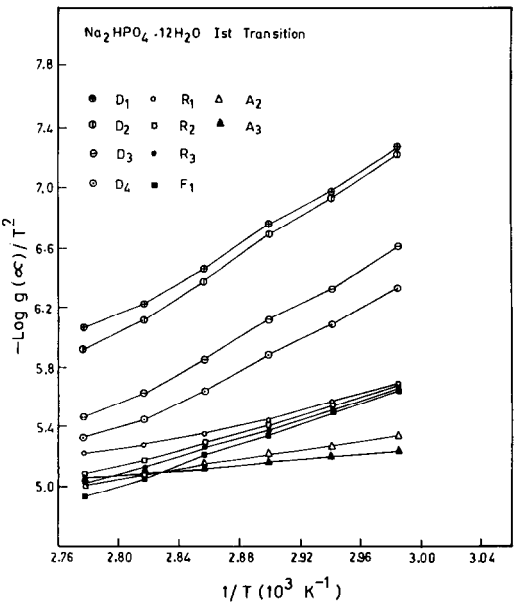

Fig. 7. Plot of $-\log[g(\alpha)/T^2]$ vs. $1/T$ for $Na_2HPO_4 \cdot 12H_2O$ (1st transition).

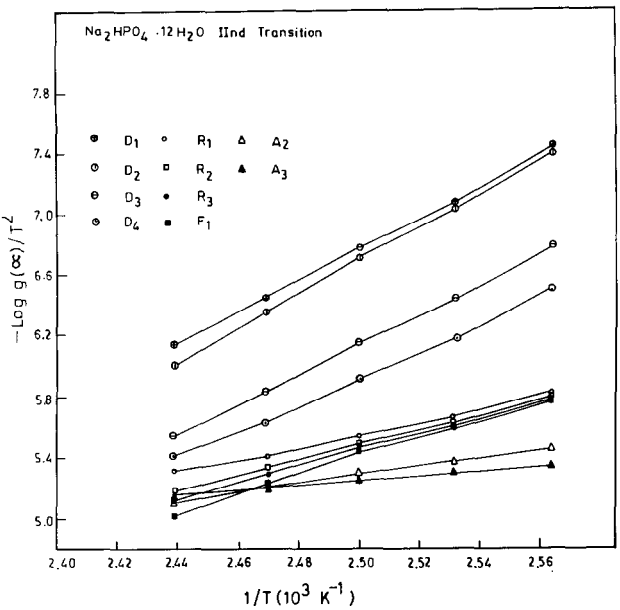

Fig. 8. Plot of $-\log[g(\alpha)/T^2]$ vs. $1/T$ for $Na_2HPO_4 \cdot 12H_2O$ (2nd transition).

nearly straight line plots. However, the deviation from linearity is more conspicuous in the diffusion mechanisms, D_1, D_2, D_3 and D_4. Under such circumstances the criterion of a straight line fit as a means of solution of the controlling mechanism is far from satisfactory. There is, therefore, a need to select some other criterion for selection of a suitable controlling mechanism for the dehydration reaction.

TABLE 3

Kinetic parameters of the dehydration of $NaCH_3COO \cdot 3H_2O$

Mechanism	Coats–Redfern	Zsako		
	E_{act} (kJ mol^{-1})	Std. dev.	E_{act} (kJ mol^{-1})	Z
R_1	33.28	0.0063	33.49	3.589×10^4
R_2	35.37	0.0063	35.58	8.017×10^4
R_3	36.04	0.0084	35.58	8.147×10^4
F_1	37.09	0.0077	37.67	1.786×10^5
A_2	15.74	0.0042	16.74	1.959×10^2
A_3	8.50	0.0069	10.46	1.365×10^1
D_1	72.58	0.0124	73.25	7.031×10^9
D_2	75.26	0.0122	75.35	7.760×10^9
D_3	78.11	0.0144	77.44	3.819×10^9
D_4	77.86	0.0138	77.44	3.647×10^9

TABLE 4

Kinetic parameters of the dehydration of $Na_2S_2O_3 \cdot 5H_2O$ (1st transition)

Mechanism	Coats–Redfern	Zsako		
	E_{act} (kJ mol^{-1})	Std. dev.	E_{act} (kJ mol^{-1})	Z
R_1	51.53	0.0276	52.32	5.861×10^7
R_2	58.98	0.0385	64.88	5.794×10^9
R_3	61.62	0.0811	73.25	1.169×10^{11}
F_1	67.14	0.0546	129.77	5.715×10^{19}
A_2	30.60	0.2628	62.79	6.138×10^9
A_3	19.72	0.1750	39.77	1.923×10^6
D_1	109.63	0.0546	110.93	1.256×10^{16}
D_2	118.60	0.0215	123.49	5.821×10^{17}
D_3	129.18	0.1628	152.79	4.074×10^{21}
D_4	124.53	0.0469	131.86	2.512×10^{18}

Zsako's method

A computer program based on Zsako's method was developed. All the controlling mechanisms reported in Table 1 were incorporated in the program. The data obtained from the TG curves were analysed by this method. The mechanisms of the dehydration process, the energy of activation E_{act} and the pre-exponential factor Z (sometimes referred to as the frequency factor) were evaluated. The results obtained using this program are reported in Tables 3–7 under the heading Zsako. It can be inferred from these results that it becomes very difficult to isolate a single mechanism on the basis of the minimum standard deviation for different mechanisms, as they are very

TABLE 5

Kinetic parameters of the dehydration of $Na_2S_2O_3 \cdot 5H_2O$ (2nd transition)

Mechanism	Coats–Redfern	Zsako		
	E_{act} (kJ mol^{-1})	Std. dev.	E_{act} (kJ mol^{-1})	Z
R_1	136.04	0.0168	136.04	1.122×10^{18}
R_2	156.43	0.0204	156.97	7.586×10^{20}
R_3	164.51	0.0278	163.25	5.370×10^{21}
F_1	180.92	0.0473	179.99	9.550×10^{23}
A_2	87.11	0.0237	87.91	4.677×10^{11}
A_3	55.80	0.0158	56.51	6.009×10^7
D_1	279.58	0.0358	246.97	1.549×10^{32}
D_2	304.78	0.0702	249.07	1.950×10^{32}
D_3	338.48	0.1451	249.07	5.248×10^{31}
D_4	312.90	0.0925	249.07	4.571×10^{31}

TABLE 6

Kinetic parameters of the dehydration of $Na_2HPO_4 \cdot 12H_2O$ (1st transition)

Mechanism	Coats–Redfern	Zsako		
	E_{act} (kJ mol^{-1})	Std. dev.	E_{act} (kJ mol^{-1})	Z
R_1	45.08	0.0170	48.14	1.574×10^7
R_2	55.00	0.0127	56.51	8.356×10^8
R_3	58.69	0.0117	58.60	1.888×10^9
F_1	66.56	0.0138	66.98	4.375×10^{11}
A_2	30.64	0.0071	31.39	1.259×10^5
A_3	18.46	0.0046	18.84	1.148×10^3
D_1	96.74	0.0337	96.28	4.898×10^{14}
D_2	109.00	0.0276	108.84	2.630×10^{16}
D_3	123.99	0.0230	123.49	1.288×10^{18}
D_4	115.16	0.0255	113.02	2.754×10^{16}

close to each other. For example, in the case of sodium acetate trihydrate, the minimum standard deviation for mechanisms R_1 and R_2 is almost the same, i.e. 0.0063; in other cases also, it is found that the difference in the minimum standard deviation is less than marginal. However, the D mechanisms have high values of the standard deviation in all these cases; therefore these can be ignored. Among the remaining mechanisms, however, the difference in the standard deviations is very small. It can also be observed from these tables that the energies of activation obtained from the Coats–Redfern method are comparable to the values obtained by Zsako's method. However, it can be noted from these tables that the value of Z varies from 10^1 to 10^{32} for different mechanisms, whereas in the case of homogeneous

TABLE 7

Kinetic parameters of the dehydration of $Na_2HPO_4 \cdot 12H_2O$ (2nd transition)

Mechanism	Coats–Redfern	Zsako		
	E_{act} (kJ mol^{-1})	Std. dev.	E_{act} (kJ mol^{-1})	Z
R_1	83.05	0.0182	87.91	7.244×10^{11}
R_2	102.77	0.0084	102.56	8.128×10^{13}
R_3	106.16	0.0086	106.74	3.162×10^{14}
F_1	119.68	0.0191	117.21	9.120×10^{15}
A_2	56.51	0.0095	56.51	7.249×10^7
A_3	35.41	0.0063	35.58	9.509×10^4
D_1	172.63	0.0363	182.09	1.202×10^{24}
D_2	193.43	0.0220	198.83	1.230×10^{26}
D_3	219.01	0.0174	219.76	2.042×10^{28}
D_4	204.07	0.0175	205.11	2.046×10^{26}

reactions, frequency factor ranges between 10^{11} and 10^{13}. It may be inferred that Z may not have the same significance as the frequency factor in kinetic equations of homogeneous reactions. In view of this, Z has been considered as a pre-exponential factor.

The reason that more than one mechanism fits the experimental data can be attributed to the fact that the equations representing these mechanisms are interrelated. The interrelation of various mechanisms can be explained by examining Table 1; it may be observed that mechanisms F_1, A_2 and A_3 can be represented by the relation

$$[\log g(\alpha)]_{F_1} = 1/2[\log g(\alpha)]_{A_2} = 1/3[\log g(\alpha)]_{A_3} \quad (8)$$

Thus, if mechanism F_1 can be represented by a straight line, then A_2 and A_3 will also generate straight lines of different slopes. The slopes of the lines representing mechanisms A_2 and A_3 will be $1/2$ and $1/3$ times the slope of the line representing mechanism F_1. Tables 3–7 also indicate that the activation energy values for mechanism F_1 are nearly double those given by mechanism A_2, and three times those of A_3. Therefore, these three mechanisms cannot be distinguished by the simple criterion of a straight line fit. The relations between the mechanisms R_3 and D_3, D_2 and R_2, and D_4 and R_3 have been reported in the literature [7,8].

In order to resolve this disparity in the results, it was decided to study the dehydration mechanism in more depth so as to find a criterion for the selection of a suitable mechanism.

CRITERION FOR THE EVALUATION OF KINETIC DATA OF SALT HYDRATES

The process of thermal decomposition of salt hydrates may be summarized by the following sequence:

$$\text{Salt hydrate(s)} \xrightarrow[\text{Step 1}]{\text{Heat}} \text{Salt hydrate(l)} \xrightarrow[\text{Step 2}]{\text{Heat}} \text{Anhydrous salt(s)} + H_2O(g) \quad (9)$$

Step 1 is the dissolution of anhydrous salt in its water of crystallization which is analogous to melting, whereas step 2 represents the loss of water of crystallization in the form of water vapour, i.e. the dehydration process.

Thermogravimetric data have been obtained for these steps. The TG records of these salt hydrates may therefore be described as the evaporation of water from the melts. It is vital to note that under these circumstances the barrier to evaporation of water from such a melt is greater than the latent heat of vaporization of water. In other words, in general, the energy of activation for step 2 in the above sequence should be more than the latent heat of vaporization of water. Understandably, we cannot use the latent heat of evaporation of pure water as a criterion for the selection of a set of

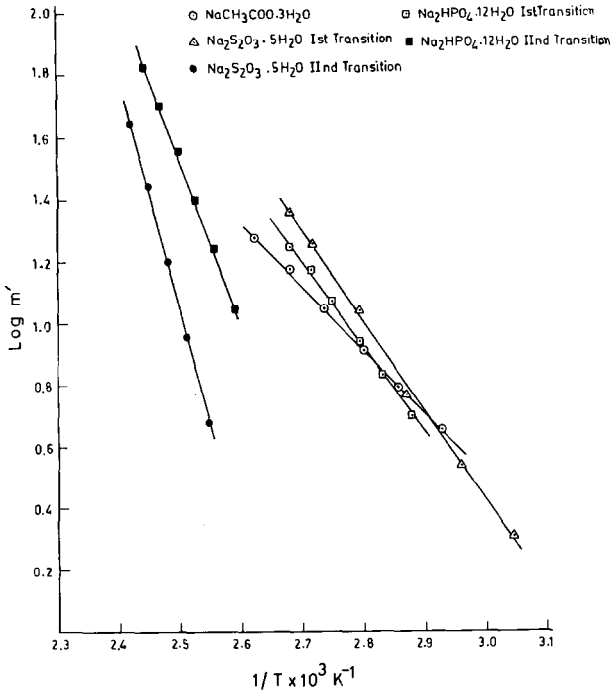

Fig. 9. Plot of log m' vs. $1/T$ for sodium salt hydrates.

physically significant values of E_{act} for the thermal decomposition of salt hydrates. In general, the aquation of an anhydrous salt is a spontaneous process and the energy of activation for the dehydration process may equal its enthalpy of dehydration. Therefore, it was thought worthwhile to determine the actual enthalpies of dehydration of the salt hydrates. Stepin et al. [9] have given a method for the evaluation of the enthalpy of dissociation of compounds. The relationship they derived to determine the enthalpy of dissociation is

$$\log m' = -(\Delta H/2.303RT) + c' \tag{10}$$

where m' is the relative weight loss with time and ΔH is the enthalpy of dissociation. This equation was used by Stepin et al. to evaluate the enthalpy of dissociation of $RbI(I)_2$.

The enthalpy of dehydration ΔH of the salt hydrates for the reaction

$$\text{Salt hydrate(s)} \rightarrow \text{Anhydrous salt(s)} + H_2O(g) \tag{11}$$

was calculated using eqn. (10) which indicates that a plot of log m' vs. $1/T$ should result in a straight line. The slope of this straight line gives the ΔH values. The plots of log m' vs. $1/T$ for various salt hydrates are shown in Fig. 9. The ΔH values for the salt hydrates are reported in Table 8. As expected, ΔH values are higher than the heat of evaporation of water

TABLE 8

Enthalpy of dehydration of sodium salt hydrates

Salt hydrate	ΔH (kJ mol^{-1})
$NaCH_3COO \cdot 3H_2O$	39.56
$Na_2S_2O_3 \cdot 5H_2O$	
First transition	57.77
Second transition	153.37
$Na_2HPO_4 \cdot 12H_2O$	
First transition	51.49
Second transition	94.56

($\Delta H = 40.60$ kJ mol^{-1}), except for $NaCH_3COO \cdot 3H_2O$ where $\Delta H = 39.56$ kJ mol^{-1}; the difference may be due to the efflorescent nature of this salt.

By comparing the values of the energy of activation of the dehydration step with the values of the enthalpy of dehydration ΔH, it can be observed that only for the mechanisms R_1, R_2, R_3 and F_1 are the values of E_{act} comparable with the values of ΔH; for the other mechanisms, the deviation is greater. On the basis of the standard deviation values for the various mechanisms reported in Tables 3–7, it can be inferred that the decomposition of salt hydrates is dictated by the Avrami–Erofeev mechanisms, as in these cases the standard deviation values are lowest, except for $Na_2S_2O_3 \cdot 5H_2O$ (first transition). However, the E_{act} values for these mechanisms are much lower than those of ΔH and should therefore be discarded in the light of the argument presented above. The standard deviations for diffusion mechanisms are comparatively high and the activation energy values are also very high compared with the ΔH values. Therefore, based on the criterion proposed above, the diffusion mechanism can also be discarded. Amongst the remaining mechanisms, the salt hydrates seem to follow the mechanisms R_1, R_2, R_3 and F_1. On the basis of the criterion $E_{act} \approx \Delta H$, the mechanisms and E_{act} values are listed in Table 9. The activation energy values are the

TABLE 9

Energy of activation E_{act} and enthalpy of dehydration (ΔH) for sodium salt hydrates

Salt hydrate	Mechanism	E_{act} (kJ mol^{-1})	ΔH (kJ mol^{-1})	Z
$NaCH_3COO \cdot 3H_2O$	F_1	37.38	39.56	1.786×10^5
$Na_2S_2O_3 \cdot 5H_2O$				
First transition	R_2	61.91	57.77	5.794×10^9
Second transition	R_2	156.68	153.37	7.586×10^{20}
$Na_2HPO_4 \cdot 12H_2O$				
First transition	R_2	55.76	51.49	8.356×10^8
Second transition	R_2	102.64	94.56	8.128×10^{13}

averages of those obtained by the methods of Coats and Redfern and of Zsako.

CONCLUSIONS

It can be concluded from the above discussion that it is possible to isolate a single mechanism to represent the dehydration process on the basis of the criterion that the energy of activation is approximately equal to the enthalpy of dehydration. The dehydration processes for sodium thiosulphate pentahydrate and disodium hydrogen phosphate dodecahydrate are governed by a two-dimensional movement of the phase boundary (R_2), whereas the dehydration process for sodium acetate trihydrate is governed by the Mampel unimolecular law (F_1). The lower energy of activation values in the case of sodium acetate trihydrate indicate that this salt hydrate is less stable than sodium thiosulphate pentahydrate and disodium hydrogen phosphate dodecahydrate.

REFERENCES

1 S.K. Sharma and C.K. Jotshi (Eds.), Proceedings of First National Workshop on Solar Energy Storage, Punjab University, Chandigarh, India, 1979.
2 M. Telkes, ASHRAE J., 9 (1974) 38.
3 J.M. Criado and A. Ortega, Int. J. Chem. Kinet., 17 (1985) 1365.
4 A.W. Coats and J.P. Redfern, Nature, 201 (1964) 68.
5 J. Zsako, J. Phys. Chem., 72 (1968) 2406.
6 C.H. Bamford and C.F.H. Tipper (Eds.), Comprehensive Chemical Kinetics, Vol. 22, Reaction in Solid State, Elsevier, New York, 1980.
7 A.M. Gadalla, Int. J. Chem. Kinet., 16 (1984) 655.
8 J.M. Criado and J. Morales, Thermochim. Acta, 19 (1977) 305.
9 B.D. Stepin, G.R. Allakherder and G.M. Serebrennikova, Russ. J. Phys. Chem., 43 (1969) 1377.

ACKNOWLEDGEMENT

This work was supported by the Department of Non-Conventional Energy Sources, Government of India.